J|A|C|S
ARTICLES
Published on Web 01/03/2004

Control of Protein Structure and Function through Surface Recognition by Tailored Nanoparticle Scaffolds

Rui Hong,[†] Nicholas O. Fischer,[†] Ayush Verma,[†] Catherine M. Goodman,[†] Todd Emrick,*[,‡] and Vincent M. Rotello*[,†]

Contribution from the Department of Chemistry and Department of Polymer Science and Engineering, University of Massachusetts, Amherst, Massachusetts 01003

Received July 22, 2003; E-mail: tsemrick@mail.pse.umass.edu; rotello@chem.umass.edu

Abstract: Thioalkyl and thioalkylated oligo(ethylene glycol) (OEG) ligands with chain-end functionality were used to fabricate water-soluble CdSe nanoparticle scaffolds. Surface recognition of chymotrypsin (ChT) was achieved using these functionalized nanoparticle scaffolds, with three levels of interaction demonstrated: no interaction (OEG terminated with hydroxyl group), inhibition with denaturation (carboxylate-terminated thioalkyl ligands), and inhibition with retention of structure (carboxylate-terminated OEG). The latter process was reversible upon an increase in ionic strength, with essentially complete restoration of enzymatic activity.

Recognition of protein surfaces using synthetic receptors is an effective strategy for regulating protein−protein and protein−substrate interactions.[1] The successful development of these receptors provides access to new classes of enzyme inhibitors,[2] protein antagonists,[3] and diagnostic biosensors.[4] These receptors can also be used to mimic[5] and interrupt[6] protein−protein and protein−DNA/−RNA interactions. However, the design of artificial scaffolds for specific recognition is complicated by the large interfacial area required (>6 nm^2 of surface area is typically buried in protein−protein interaction[7]) and by the complex topology[8] of hydrophobic,[9] electrostatic,[10] and polar residues located on the protein surface.

Monolayer-protected colloidal nanoparticles provide a versatile scaffold for protein surface recognition due to their size (commensurate with proteins), the ability to tailor monolayer surfaces with a wide range of functionalities,[11] and the templatability of the surface monolayer.[12] Furthermore, the utility of these particles is enhanced by the range of core materials available, including metal, semiconductor, or oxide core materials that exhibit useful electronic,[13] fluorescence,[14] and magnetic properties.[15] In our previous work[16] we used mercaptoundecanoic acid (MUA) functionalized gold nanoparticles to target α-chymotrypsin (ChT) through electrostatic interactions between the anionic particle surface and the cationic "hot spot" around the ChT active site.[17] Binding of the particles resulted in enzymatic inhibition, followed by denaturation of ChT, presumably due to hydrophobic interactions with the alkyl interior of the monolayer. The MUA−Au system and other recently reported synthetic receptors[18] bind irreversibly to the target protein and destabilize or denature the native structure of the protein. However, there is a need to retain the native structure upon protein binding in applications such as in vivo protein delivery[19] and in vitro enzyme stabilization.[20] Also, effective templation of monolayers[12] to protein surfaces will require retention of native protein structure.

We have explored the use of oligo(ethylene glycol) (OEG) terminated monolayers to provide access to noninteracting particles as well as systems featuring controlled protein surface interactions.[21] We report here the design of functional ligands composed of thioalkylated OEG with chain-end recognition elements and the use of functionalized nanoparticle scaffolds

[†] Department of Chemistry.
[‡] Department of Polymer Science and Engineering.

(1) Peczuh, M. W.; Hamilton, A. D. *Chem. Rev.* **2000**, *100*, 2479−2493.
(2) Park, H. S.; Lin, Q.; Hamilton, A. D. *J. Am. Chem. Soc.* **1999**, *121*, 8−13.
(3) Zutshi, R.; Franciskovich, J.; Shultz, M.; Schweitzer, B.; Bishop, P.; Wilson, M.; Chmielewski, J. *J. Am. Chem. Soc.* **1997**, *119*, 4841−4845.
(4) Ratner, B. D. *J. Mol. Recognit.* **1996**, *9*, 617−625.
(5) Mahtab, R.; Rogers, J. P.; Singleton, C. P.; Murphy, C. J. *J. Am. Chem. Soc.* **1996**, *118*, 7028−7032.
(6) Park, H. S.; Lin, Q.; Hamilton, A. D. *Proc. Natl. Acad. Sci. U.S.A.* **2002**, *99*, 5105−5109.
(7) Stites, W. E. *Chem. Rev.* **1997**, *97*, 1233−1250.
(8) Mammen, M.; Choi, S. K.; Whitesides, G. M. *Angew. Chem., Int. Ed.* **1998**, *37*, 2755−2794.
(9) Lijnzaad, P.; Argos, P. *Proteins* **1997**, *28*, 333−343.
(10) Golumbfskie, A. J.; Pande, V. S.; Chakraborty, A. K. *Proc. Natl. Acad. Sci. U.S.A.* **1999**, *96*, 11707−11712.
(11) Templeton, A. C.; Wuelfing, M. P.; Murray, R. W. *Acc. Chem. Res.* **2000**, *33*, 27−36.
(12) Boal, A. K.; Rotello, V. M. *J. Am. Chem. Soc.* **2000**, *122*, 734−735.
(13) Shipway, A. N.; Katz, E.; Willner, I. *ChemPhysChem* **2000**, *1*, 18−52.
(14) Alivisatos, A. P. *Science* **1996**, *271*, 933−937. Nirmal, M.; Brus, L. *Acc. Chem. Res.* **1999**, *32*, 407−414. Murphy, C. J. *Anal. Chem.* **2002**, *74*, 520a−526a. Trindade, T.; O'Brien, P.; Pickett, N. L. *Chem. Mater.* **2001**, *13*, 3843−3858. Chan, W. C. W.; Maxwell, D. J.; Gao, X. H.; Bailey, R. E.; Han, M. Y.; Nie, S. M. *Curr. Opin. Biotechnol.* **2002**, *13*, 40−46.
(15) Safarik, I.; Safarikova, M. *Monatsh. Chem.* **2002**, *133*, 737−759.
(16) Fischer, N. O.; McIntosh, C. M.; Simard, J. M.; Rotello, V. M. *Proc. Natl. Acad. Sci. U.S.A.* **2002**, *99*, 5018−5023. Fischer, N. O.; Verma, A.; Goodman, C. M.; Simard, J. M.; Rotello, V. M. *J. Am. Chem. Soc.* **2003**, *125*, 13387−13391.
(17) Bogan, A. A.; Thorn, K. S. *J. Mol. Biol.* **1998**, *280*, 1−9. Capasso, C.; Rizzi, M.; Menegatti, E.; Ascenzi, P.; Bolognesi, M. *J. Mol. Recognit.* **1997**, *10*, 26−35.
(18) Wilson, A. J.; Groves, K.; Jain, R. K.; Park, H. S.; Hamilton, A. D. *J. Am. Chem. Soc.* **2003**, *125*, 4420−4421. Jain, R. K.; Hamilton, A. D. *Angew. Chem., Int. Ed.* **2002**, *41*, 641−643.
(19) Sood, A.; Panchagnula, R. *Chem. Rev.* **2001**, *101*, 3275−3303.
(20) O'Fagain, C. *Enzyme Microb. Tech.* **2003**, *33*, 137−149.
(21) Rosenthal, S. J.; Tomlinson, A.; Adkins, E. M.; Schroeter, S.; Adams, S.; Swafford, L.; McBride, J.; Wang, Y. Q.; DeFelice, L. J.; Blakely, R. D. *J. Am. Chem. Soc.* **2002**, *124*, 4586−4594. Skaff, H.; Emrick, T. *Chem. Commun.* **2003**, 52−53.

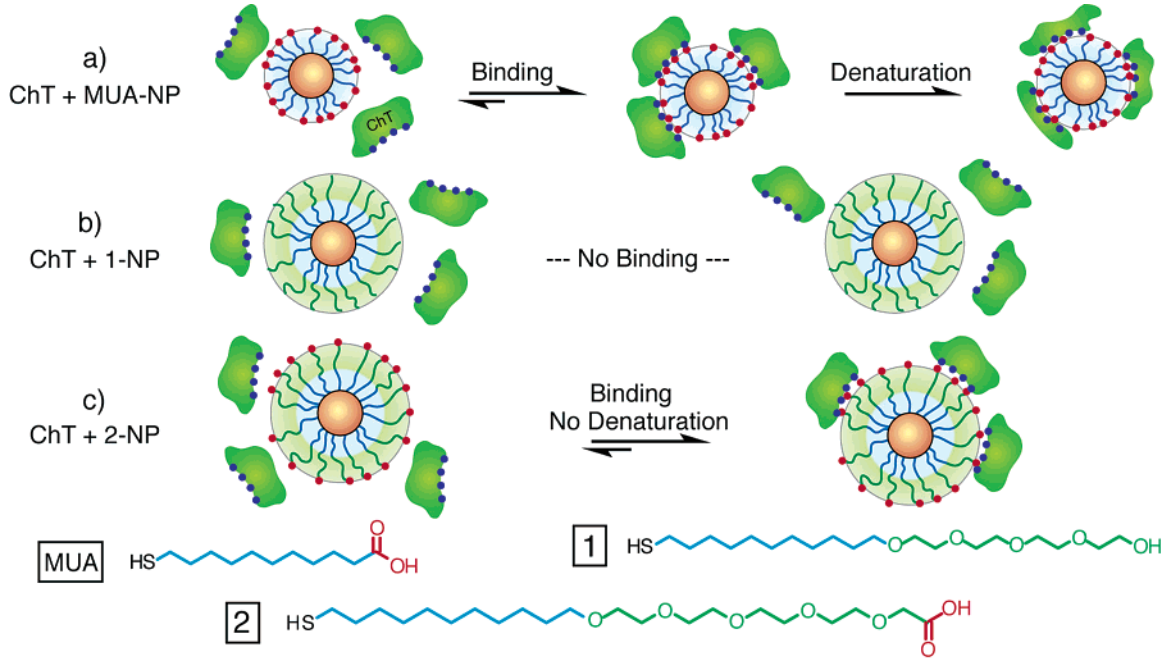

Figure 1. Ligands used for CdSe nanoparticles, and schematic depiction of protein−nanoparticle interactions.

to target chymotrypsin. Three levels of control over ChT structure and function were achieved with these surface functionalized particles (Figure 1): (a) binding and denaturation with MUA-NP, (b) no binding with **1**-NP, and (c) binding and retention of the protein structure with **2**-NP.

Results and Discussion

Fabrication of Nanoparticle Scaffolds. CdSe nanoparticles featuring a 3.2 ± 0.3 nm core[22] were functionalized with thioalkylated tetra(ethylene glycol) (EG4) ligands **1** and **2** and MUA to give water soluble CdSe particles (**1**-NP, **2**-NP, and MUA-NP, respectively) through a facile ligand exchange reaction (see Supporting Information). Ligand **1** features a neutral hydroxyl end group and is generally bioinert.[23] Although no charges are present on the surface, **1**-NP is highly water-soluble.[24] The terminal carboxylate functionality in **2**-NP acts as the recognition element, targeting the cationic patch surrounding the active site of the ChT surface via charge complementarity. Integration of OEG and recognition functionalities into the same ligand molecule is interesting from several perspectives. First, the resistance of nonspecific protein adsorption by OEG should increase the biospecificity of the recognition, as has been shown on 2D surfaces.[25,26] Second, highly hydrophilic OEG spacer prevents hydrophobic interactions between proteins and the hydrophobic monolayer interior, thus aiding in the retention of protein structure. Third, the combination of protein binding with retention of its structure and the subsequent release of the protein makes the nanoparticle scaffolds promising for protein delivery and protein modification.[20] Finally, the similar solubility and reactivity of these thiol OEG ligands make one-pot ligand exchange possible on both CdSe and Au nanoparticles. As the use of CdSe-based nanoparticles as fluorescent tags for bioimaging is a topic of considerable current interest,[27] our system provides a model to better understand and control the interactions between CdSe nanoparticles and proteins.

ChT Activity Assays. The formation of ChT−nanoparticle complexes through charge complementarily was first confirmed by gel electrophoresis experiments (Figure 2a). No migration was observed for **1**-NP, which is consistent with its neutral surface functionality. Upon addition of ChT, mobility shifts of the charged NP species (MUA and **2**-NP) were observed, attributed to both an increase in size and an attenuation of the particle surface charge due to ChT binding and complex formation. At a 4:1 ratio of ChT:nanoparticle, a fraction of unbound **2**-NP was observed in the gel (line 7 of Figure 2a). In previous work,[16] complete inhibition of ChT using 6 nm MUA−Au scaffolds was observed at a ChT:nanoparticle binding ratio of 4:1. The current **2**-NP scaffold diameter is larger than the MUA-Au system by approximately 4 nm (3 nm CdSe core + ~7 nm for the C_{11} alkyl-EG4 chain), with a concomitant increase in surface area of ~3-fold. Addition of ChT in incremental steps (Figure 2b) shows that no free nanoparticles are seen at ChT:**2**-NP ratios greater than 12:1, consistent with

(22) Aldana, J.; Wang, Y. A.; Peng, X. G. *J. Am. Chem. Soc.* **2001**, *123*, 8844−8850. Peng, Z. A.; Peng, X. G. *J. Am. Chem. Soc.* **2001**, *123*, 183−184.
(23) For chemical reactivity of these systems, see: Pathak, S.; Choi, S. K.; Arnheim, N.; Thompson, M. E. *J. Am. Chem. Soc.* **2001**, *123*, 4103−4104.
(24) Most of the previously reported water soluble semiconductor nanoparticles present charge on the surface. See: Mattoussi, H.; Mauro, J. M.; Goldman, E. R.; Anderson, G. P.; Sundar, V. C.; Mikulec, F. V.; Bawendi, M. G. *J. Am. Chem. Soc.* **2000**, *122*, 12142−12150. Willard, D. M.; Carillo, L. L.; Jung, J.; Van Orden, A. *Nano Lett.* **2001**, *1*, 469−474. Wang, S. P.; Mamedova, N.; Kotov, N. A.; Chen, W.; Studer, J. *Nano Lett.* **2002**, *2*, 817−822. Reference 25c.
(25) Mrksich, M.; Whitesides, G. M. In *Poly(ethylene glycol): Chemistry and Biological Applications*; Harris, M. J., Zalipsky, S., Eds.; American Chemical Society: Washington, DC, 1997; pp 361−373. Kane, R.; Deschatelets, P.; Whitesides, G. M. *Langmuir* **2003**, *19*, 2388−2391 and references therein.
(26) Mrksich, M.; Grunwell, J. R.; Whitesides, G. M. *J. Am. Chem. Soc.* **1995**, *117*, 12009−12010.
(27) (a) Sutherland, A. J. *Curr. Opin. Solid State Mater.* **2002**, *6*, 365−370. (b) Bruchez, M.; Moronne, M.; Gin, P.; Weiss, S.; Alivisatos, A. P. *Science* **1998**, *281*, 2013−2016. (c) Chan, W. C. W.; Nie, S. M. *Science* **1998**, *281*, 2016−2018. (d) Akerman, M. E.; Chan, W. C. W.; Laakkonen, P.; Bhatia, S. N.; Ruoslahti, E. *Proc. Natl. Acad. Sci. U.S.A.* **2002**, *99*, 12617−12621. (e) Dubertret, B.; Skourides, P.; Norris, D. J.; Noireaux, V.; Brivanlou, A. H.; Libchaber, A. *Science* **2002**, *298*, 1759−1762. (f) Jaiswal, J. K.; Mattoussi, H.; Mauro, J. M.; Simon, S. M. *Nat. Biotechnol.* **2003**, *21*, 47−51.

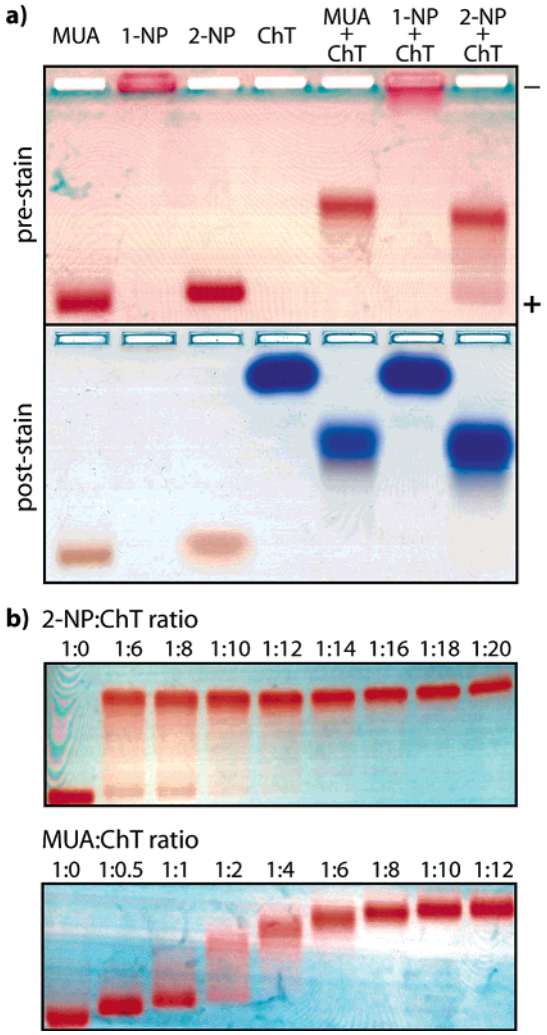

Figure 2. Gel electrophoresis of ChT and nanoparticles. (a) Nanoparticle interactions with ChT, before and after protein staining. ChT:nanoparticle ratios were held constant at 4:1 ([ChT] = 50 μM; [nanoparticle] = 12.5 μM). (b) Determination of binding stoichiometry. **2**-NP concentrations were varied at a constant ChT concentration (50 μM), while MUA concentrations were held constant at 6.0 μM at various ChT concentrations. Results after protein staining for these two gels are provided in the Supporting Information.

our predictions. The narrow band observed for the ChT−**2**-NP complex indicates the formation of discrete complexes, as opposed to extended ChT−nanoparticle aggregates. From similar experiments, the binding ratio of ChT to MUA-NP is approximately 6:1, which is also consistent with the size of the MUA-NP scaffold (3 nm CdSe core + 4 nm for C_{11} monolayer, resulting in a ~50% increase in surface area).

The binding of ChT to nanoparticles decorated with terminal carboxylates (MUA-NP and **2**-NP) resulted in the rapid and essentially complete inhibition of ChT hydrolysis of *N*-succinyl-L-phenylalanine-*p*-nitroanilide (SPNA; Figure 3). In contrast, **1**-NP had no effect on the activity of ChT, demonstrating that protein adsorption on the EG4 surface is unfavorable.

The inhibition by MUA-NP (CdSe) is very similar to that of the previously reported MUA−Au system. This confirms the critical role of a particular ligand environment to control the properties of multiple nanoparticle compositions. As expected from electrophoresis experiments, **2**-NP also efficiently inhibited ChT activity (Figure 4). Further activity assays by using different

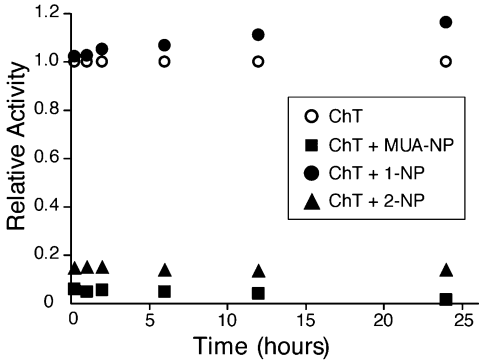

Figure 3. Normalized activity of ChT (3.2 μM) with nanoparticles (0.8 μM).

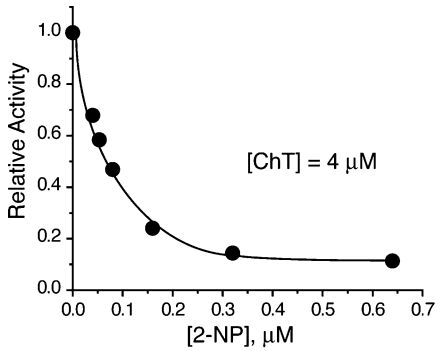

Figure 4. Dose-responsive inhibition of ChT by **2**-NP. Trend line was added to guide the eye.

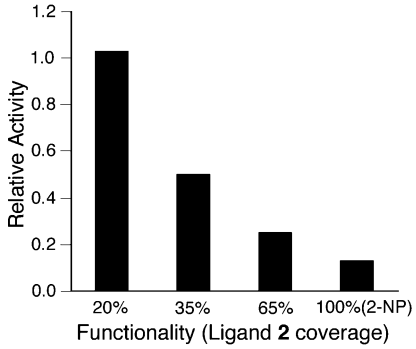

Figure 5. Normalized activity of ChT (3.2 μM) with MMNPs and **2**-NP (0.8 μM).

2-NP concentrations reveal that the inhibition is efficient, with an 85% inhibition of ChT activity observed at a ChT:nanoparticle ratio of 12.5. Further increase of **2**-NP concentration does not significantly increase the degree of inhibition, in agreement with the binding ratio obtained from gel electrophoresis.

The relative coverage of EG4−carboxylic acid functionality (ligand **2**) had a significant impact on the potency of the inhibition. Nanoparticles featuring mixed monolayers composed of ligands **1** and **2** (MMNPs) were synthesized via a one-pot ligand-exchange reaction. The percentage of EG4−COOH ligand **2** was varied from ~20% (MMNP1) to ~35% (MMNP2) to ~65% (MMNP3) (see Supporting Information). As shown in Figure 5, an increased density of carboxylic acid ligand **2** results in more efficient inhibition. These results suggest that a high density of functionality is required for effective protein surface binding,[1] as opposed to specific ligand recognition, which requires much lower functionality coverage.[28]

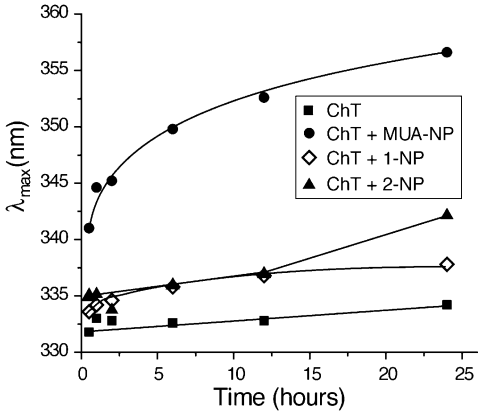

Figure 6. Tryptophan fluorescence of ChT (3.2 μM) and ChT with nanoparticles (0.8 μM). Trend lines were added to guide the eye.

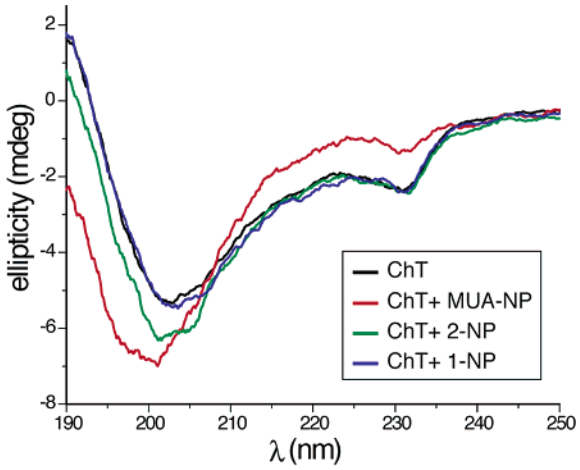

Figure 7. CD of ChT (3.2 μM) and ChT with nanoparticles (0.8 μM) after 24 h incubation.

Conformational Analysis. The structure of ChT upon binding nanoparticles was monitored by both tryptophan fluorescence and circular dichroism (CD). As shown in Figure 6, a red shift in the ChT fluorescence maximum (~20 nm in 24 h) was observed upon incubation of ChT with MUA-NP. The red shift is attributed to the exposure of tryptophan residues to more polar environments as a consequence of protein denaturation.[29] Essentially no red shift of ChT was observed with **1**-NP, indicating no interaction between ChT and the bioinert monolayer of **1**-NP. As hydroxyl-terminated nanoparticles have been shown not to bind to cells,[23] our findings provide molecular "resolution" of this behavior. Importantly, although **2**-NP inhibits ChT enzymatic activity, only a negligible red shift in the ChT fluorescence maxima was observed, which is in sharp contrast to that of ChT incubated with MUA-NP. These results suggest retention of the ChT native structure, which we attribute to the ability of the EG4 spacer to prevent hydrophobic interactions between ChT and **2**-NP.

Circular dichroism (CD) provides more detailed insight into the effect of nanoparticle binding on the secondary structure of ChT (Figure 7). As expected, no change in the CD spectrum of ChT was observed with EG4−OH-terminted particle **1**-NP, further demonstrating the bioinert nature of this surface. As

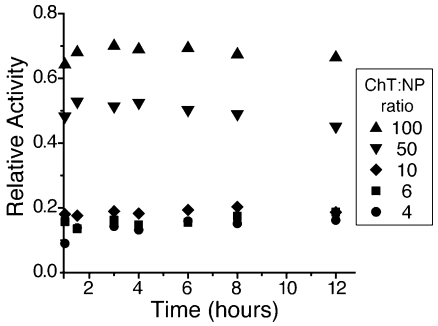

Figure 8. Time-independent inhibition of ChT by **2**-NP at different ChT: nanoparticle ratios ([ChT] = 3.2 μM).

observed previously with the Au analogue,[16] binding of ChT by MUA-NP resulted in a time-dependent loss of the characteristic minimum at 232 nm [30] and a blue shift of the minimum at 204 nm. In contrast, very little change in the CD spectrum of ChT occurred with the ChT-inhibiting particle **2**-NP over the same time frame. The retention of the ChT structure with **2**-NP upon binding is consistent with inhibition of ChT by **2**-NP through spatial blocking of the active site via electrostatic interactions, as opposed to the loss of activity due to denaturation or other major structural changes as observed with MUA-NP.

Protein Release Using Increased Ionic Strength. To determine the potential suitability of **2**-NP for delivery applications, the inhibition of ChT by **2**-NP was monitored at different ratios of ChT and **2**-NP over 12 h (Figure 8). The inhibition was determined to be time-independent, in contrast to the previously reported two-step inhibition by the MUA−Au system.[16] This time-independent inhibition, coupled with our spectroscopic studies, suggests the binding is driven primarily by electrostatic interactions and involves very little hydrophobic interactions. Consistent with this hypothesis, the binding of ChT to **2**-NP was found to be highly reversible. As shown in Figure 9a, when the ionic strength of the buffer was increased to 100 mM (using NaCl), **2**-NP shows no inhibition of ChT activity. However, a certain degree of inhibition was observed by MUA-NP, suggesting a role of hydrophobic interaction in the binding. In fact, essentially complete restoration of the activity of ChT inhibited by **2**-NP was achieved through disruption of the electrostatic interactions through increased ionic strength (Figure 9b). In this experiment, a NaCl stock solution was added to a preincubated (>1 h) solution of ChT and **2**-NP. The enzymatic activity of ChT was recovered as the ionic strength of the solution was increased, resulting in an essentially full recovery at a NaCl concentration of 100 mM. The rescue of the ChT activity is consistent with the release of protein from the **2**-NP surface as a direct result of attenuating the electrostatic interactions between ChT and **2**-NP.

Conclusions

In summary, we have demonstrated control over both protein structure and function through surface recognition by tailored nanoparticle scaffolds. Using alkanethiol−carboxylate functionalized MUA-NP, binding, inhibition, and denaturation of ChT were observed. The tetraethylene glycol spacer between the alkyl chain and recognition element in **2**-NP allowed reversible electrostatic interactions between the particle and

(28) Roberts, C.; Chen, C. S.; Mrksich, M.; Martichonok, V.; Ingber, D. E.; Whitesides, G. M. *J. Am. Chem. Soc.* **1998**, *120*, 6548−6555.
(29) Ladokhin, A. S. In *Encyclopedia of Analytical Chemistry*; Meyers, R. A., Ed.; John Wiley & Sons Ltd.: Chichester, U.K., 2000; pp 5762−5779.
(30) Cantor, C. R.; Timasheff, S. N. In *The Proteins*, Vol. V; Neurath, H., Hill R. L., Eds.; Academic Press Inc.: New York, 1982; pp 145−305.

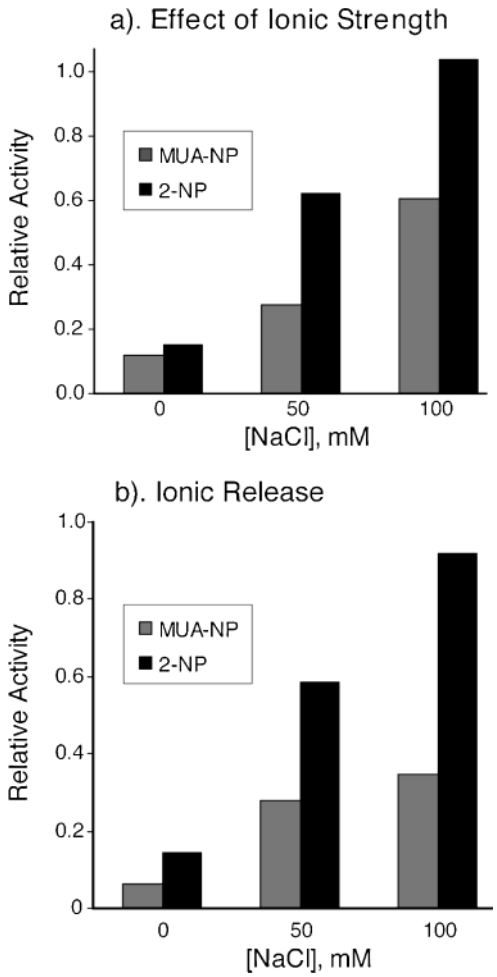

Figure 9. Reversibility of ChT binding to **2**-NP. (a) The ionic strength of ChT solution was increased by adding NaCl stock solution to the desired concentration before adding nanoparticle solution; (b) ChT was incubated with nanoparticles in normal 5 mM phosphate buffer for 1 h before increasing the ionic strength.

protein, but prevented the hydrophobic interactions between ChT and the alkyl interior of the monolayer. As a result, efficient reversible inhibition was observed without protein denaturation. The binding can be tuned by either varying the percentage of the recognition elements on the particles or increasing the ionic strength of the solution. Finally, **1**-NP, lacking the carboxylate recognition element, was inert to protein interaction. Overall, we have demonstrated that incorporation of OEG and recognition elements onto monolayer protected nanoparticles provides a versatile scaffold to bind biomolecules. The reversibility of the bound protein in **2**-NP systems provides new opportunities for protein stabilization, modification, and delivery; further explorations of these applications are underway.

Experimental Section

Materials. Cadmium acetate (99.999%), selenium powder, tri-*n*-octylphosphine (TOP), and tri-*n*-octylphosphine oxide (TOPO) were purchased from Alfa Aesar. α-Chymotrypsin from bovine pancreas (EC 3.4.21.1) and SPNA were purchased from Sigma. All the other chemicals were obtained from Aldrich. All the solvents were purchased from VWR and were used as received unless specified otherwise.

Activity Assays. Enzymatic activity assays were preformed using a microplate reader (EL808IU, Bio-Tek Instruments, Winooski, VT). All the experiments were performed in 5 mM sodium phosphate buffer at pH = 7.4 with [ChT] = 3.2 μM, [nanoparticle] = 0.8 μM unless otherwise specified. The enzymatic hydrolysis reaction was initiated by adding a SPNA stock solution (15 μL) in EtOH to a preincubated ChT−nanoparticle solution (185 μL) to reach a final SPNA concentration of 2 mM. Hydrolysis of SPNA was monitored for 10−30 min at 405 nm. The assays were performed in duplicates or triplicates, and the averages are reported. The standard deviation was usually less than 10%.

Electrophoresis. Agarose gels were prepared in 5 mM sodium phosphate buffer at 1% final agarose concentration. Appropriately sized wells (40 μL) were formed by placing a comb in the center of the gel. A ChT stock solution of 100 μM in 5 mM sodium phosphate buffer (pH 7.4) was used to prepare 30 μL samples at the appropriate ChT: nanoparticle ratios. After a 30 min incubation period at room temperature, 3 μL of 80% glycerol was added to ensure proper well loading (30 μL,) and a constant voltage (100 V) was applied for 30 min for sufficient separation. Gels were placed in staining solution (0.5% Coomassie blue, 40% methanol, 10% acetic acid aqueous solution) for 1 h, followed by extensive destaining (40% methanol, 10% acetic acid aqueous solution) until protein bands were clear. Gels were scanned on a flatbed scanner both prior to and after staining to separately visualize particle and ChT bands.

Fluorescence and CD. For fluorescence experiments, ChT was excited at 295 nm, and the emission was recorded from 300 to 450 nm on a Shimadzu RF-5301 PC spectrofluorometer, using 10 mm quartz cuvettes. CD experiments were performed on a Jasco J-720 spectrometer, using a quartz cuvette with a 1 mm path length. Three scans were taken for each sample from 190 to 250 nm at a rate of 20 nm/min. All the experiments were performed at a constant temperature of 20 °C with a 5 min equilibration before the scans. All the fluorescence and CD experiments were performed in identical conditions as activity assays (5 mM sodium phosphate buffer, pH 7.4; [ChT] = 3.2 μM; [nanoparticle] = 0.8 μM).

Acknowledgment. This research was supported by the National Institutes of Health (Grant GM 62998, V.M.R.), and a National Science Foundation Career Award (Grant CHE-0239486, T.E.). N.O.F. acknowledges support from the NIH CBI Training Grant GM08515.

Supporting Information Available: Synthesis of ligand **2** and **1**-NP and **2**-NP, ^{1}H NMR of OEG ligand covered nanoparticles, gel electrophoresis image after protein staining in Figure 2b (PDF). This material is available free of charge via the Internet at http://pubs.acs.org.

JA037470O